IOSR Journal of Applied Physics (IOSR-JAP)
e-ISSN: 2278-4861.Volume 11, Issue 6 Ser. I (Nov. – Dec. 2019), PP 35-40
www.iosrjournals.org

Effect of Different Concentrations of Zinc Acetate on the Structural, and the Optical and Electrical Conductivity of ZnO Nanostructures

[1] A. B. Awatif*, [2]Mubarak Dirar Abdallah, [3] Abdalsakhi S M.H , [4] E.M. Elssfah
[5]Aldesogi Omer Hamed , [6]Rawia Abd Elgani Elobaid
[1,2,6]Sudan University of Science &Technology-College of Science-Department of Physics-Khartoum- Sudan
[3-5] Al-Neenlen University – Faculty of Science and Technology Department of Physics- Khartoum- Sudan
[4] Gadarif University Faculty of Engineering-Department of Physics –Gadarif-Sudan
Corresponding Author: A. B. Awatif

***Abstract**: In his paper zinc oxide Nonocomposites thin films were deposited on ITO glass substrate. Ten samples of zinc oxide were prepared by sol-gel method/thin films at different concentrations 0.1 ,0.2 ,0.3 ,0.4 ,0.5 ,0.6 ,0.7 ,0.8 ,0.9 and 1.0 molar of zinc acetate. The nanostructures/ films were characterized by X-ray diffraction and Fourier Transformer Infrared (FTIR. The UV-VIS spectrum was used to calculate the optical and electrical conductivity. The results of XRD show the effect of zinc acetate concentration on the d- spacing for as-synthesized samples Zinc Oxide (ZnO) , which indicate that the d-spacig increases when increasing the molar concentration with rate of 0.026 ^{o}A .mol^{-1}. Moreover the crystalline size increases with decreasing the ZnO concentration by rate 156.28 nm.mlo^{-1}. The FTIR rsulted that the mean band around 1340 cm^{-1} is associated with the O-H bending vibration. The results confirmed that low electrical condictivity match the high concentration zinc acetate nanostructured ZnO / ITO.*

***Keywords:** ITO glass substrate, XRD technique, optical conductivity, FTIR*

Date of Submission: 13-11-2019 Date of Acceptance: 27-11-2019

I. Introduction

Among metal oxide semiconductors, ZnO is increasingly recognized as a suitable alternative due to its richest range of morphologies among the wide band gap semiconductors (3.37 eV) and relatively lower cost of production [1,2]. ZnO was also reported to exhibit higher quantum efficiency and photocatalytic activity than TiO_2 in certain cases [3]. It has been demonstrated that ZnO nanostructures exhibit antimicrobial activity against on a broad spectrum of bacteria including Staphylococcus auerus [4] and Escherichia coli [5,6,7]. ZnO nanoparticles seem to have relative toxicity to bacteria but exhibit minimal effect on human cells [4]. The disruption of the cell membrane is attributed to peroxidation of the unsaturated phospholipids due to photocatalytically induced hydrogen peroxide [8]. Cell membrane and wall damage upon the contact with ZnO nanoparticles occur to inhibit bacterial growth [4,5]. In addition, binding Zn^{2+} ion to the membranes of microorganisms results in prolong the lag phase of the microbial growth cycle [9]. A recent toxicology study by Poynton et al. [10,11] suggested that both ZnO nanoparticles and Zn^{2+} are toxic, but have different modes of action. ZnO nanostructures has many potential applications, such as light emitting lasers and diodes, piezoelectric devices and photo catalysts [12, 13], gas and chemical sensors [14], solar cell [15], ultraviolet detector [16] and biomolecular sensors [17].

The deposition of high quality Zno thin films is reported using a wide variety of techniques, such as, sputtering [18], chemical vapor deposition [19], spray pyrolysis [20], sol-gel method [21], and electrochemical deposition [22]. The sol- gel chemical deposition technique is very attractive as it can be entrenched easily in laboratory for the deposition of semiconducting thin ilms [18].

In this study ,we demonstrated a low-cost sol-gel method, by using glass substrates and spin coating technique to prepare ZnO/ITO filims nanoparticles with the use of different concentrations /molar of zinc acetate. Moreover, the effects of the different concentrations on the structural and the electrical conductivity were investigated. The most important advantages of this approach , in comparison the different of the molar concentration on the electrical properties of ZnO nanostructure. The samples were characterized by XRD, FTIR and UV-visible spectroscopy.

II. Samples Preparation:

The precursors used in the synthesis ZnO in different concentration molar seed layers by sol-gel process are Zinc acetate dehydrate $Zn(CH_3COOH)_2.2H_2O$. The need for surfactant is fulfilled by the use of 2-methoxyethanol (ME) $CH_3OCH_2CH_2OH$. The stock solution for the samples was prepared by using Zinc acetate in different molar (0.1.0 ,0.2 ,0.3 , 0.4 ,0.5 ,0.6 , 0.7 ,0.8 ,0.9 and 1.0 molar). Each molar of zinc acetate was dissolved in 100 ml of ethanol in the glass beaker. Then these solution were stirred for 60 min at 80°C to get milky solution. Then some drops of 2-methoxyethanol (ME) was added carefully to the milky solution as stabilizer to abtain a transparent solution. Finally the Zinc oxide solution has been got. The ten mounts of the samples have been leaved in the laboratory at room temperature for about 24 hours. Then the samples were washed by distilled water to obtain the Sol. The sol-gel for each sample was used to prepare the film by spinner (spin coating). The films were prepared in ITO glass slide. The ITO glass were cleaned with ethanol before, washing with deionizer water and acetone. The coating of the films on ITO glass was performed at room temperature, with suitable speed rate for 60 s. The optical conductivity and electrical condactivity of ZnO thin films sample were measured as a function of wavelength by UV-visible spectroscopy. The Fourier Transform Infrared Spectrophotometer (FTIR) in the range of 400 to 4000 cm^{-1} used to recorde some location of the band positions(spinel structure) as wavenumber function. The crystal structure of the samples were characterized at room temperature by using a Philips PW1700 X-ray diffract meter .

III. Results and Discussion

The crystal structure of the ten samples were characterized at room temperature by using a Philips PW1700 X-ray diffract meter (operated at 40 kV and current of 30 mA). The samples were scanned between 0° and 120° at a scanning speed of 0.06 $^oC/s$ using Cu Kα radiation with λ = 1.5418Å. The X-ray diffraction patterns of the as-synthesized of ZnO nanocrystals have been shown in Fig (1). The existence of the (111), (200), (220), (222), (400), (331), and (420) major lattice planes in the XRD patterns confirmed that the as-obtained ZnO nanoparticles is spinal cubic structure.

Table(1) exhbited some crystallite lattice parameters ,size , d – spacing and miller indices of the peaks shown in figure 1. According to the XRD results, the ZnO nanoparicles obtained with different concentration of zinc acetate possess high crystallinity, due to their very sharp diffraction peaks. More over no other peaks were detected which implies high purity of as-synthesized ZnO nanostructures.

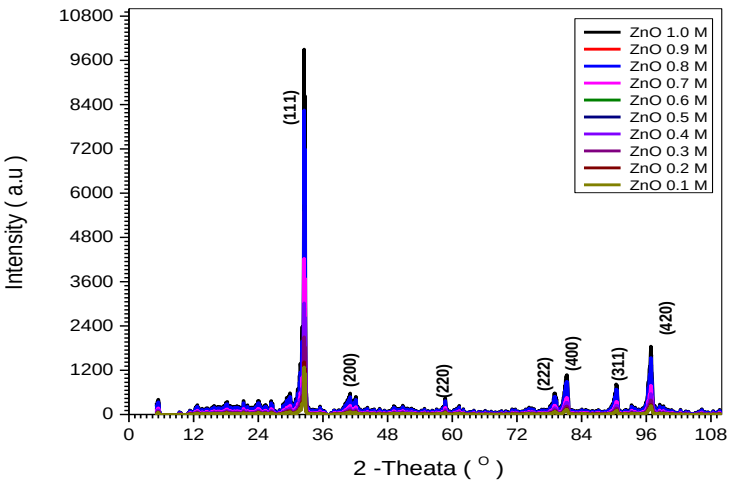

Figure (1): shows the XRD patttern of the ten ZnO sample in different concentration of zinc acetate.

Table(1): displays some crystallite lattice parameters (size , d – spacing and miller indices) of ten ZnO sample.

2-Theta	d(A)	h	k	l
33.5027	2.67255	1	1	1
38.8784	2.31450	2	0	0
56.1542	1.63660	2	2	0
78.4007	1.33628	2	2	2
83.4586	1.15725	4	0	0
92.9933	1.06197	3	3	1
96.1770	1.03508	4	2	0

Table (2) shows some crystallite lattice parameters (c- form , a,b,c, β,α, γ, density ,Xs(nm) and d – spacing) of all samples of as- sythesized ZnO nanoparticle by using different concentration of Zinc acetate. The dislocation density (δ) of the samples is calculated and listed in table (2). As can be seen from table (2) , the dislocation density increase when the concentration of ZnO molars increase. This result may lead to increase the growth of the crystal. As shown in Figure (2) the density (δ) of ZnO nanoparticles at different concentration increasing as the concentration increase by rate 10^{-3}(g.cm^{-3}) .mol^{-1} . This result can be explained as follows; when the ZnO ratio increases, it leads in increasing in the proportion of surface atoms. Figure (3) shows the relation between d- spacing and the effect of concentration in as-synthesized ZnO nanoparticles. It's noticed that the d- spacing decreased when increasing the concentration of ZnO by rate (0.026 ^{o}A .mol^{-1}).The increasing of the d- spacing is lead to the construction of larger clusters. The d- spesing decreases with increasing the ZnO concentration by rate (0.026 ^{o}A .mol^{-1}). Also the slow decrease of d-spesing in the early stage of calcinations of ZnO is attributed to prevent rapid growth of crystals.

Table (2), shows XRD parameters of ZnO nanocrystals at various crystalline orientations.

Sample	C-form	a=b=c	α= β = γ	Density	Xs(nm)	d-spesing	Average L-C
ZnO 1.0 M	Cubic	8.3981	90	5.4495	20.10	2.1433	25.4
ZnO 0.9 M	Cubic	8.3981	90	5.4494	26.93	2.1532	26.03
ZnO 0.8 M	Cubic	8.3981	90	5.4493	23.28	2.1548	27.68
ZnO 0.7 M	Cubic	8.3981	90	5.4492	24.25	2.1587	29.11
ZnO 0.6 M	Cubic	8.3981	90	5.4491	68.47	2.1608	29.21
ZnO 0.5 M	Cubic	8.3981	90	5.4490	92.15	2.1623	30.66
ZnO 0.4 M	Cubic	8.3981	90	5.4489	108.55	2.1654	36.75
ZnO 0.3 M	Cubic	8.3981	90	5.4488	114.83	2.1672	38.41
ZnO 0.2 M	Cubic	8.3981	90	5.4487	129.53	2.1687	39.34
ZnO 0.1 M	Cubic	8.3981	90	5.4486	145.23	2.1697	39.35

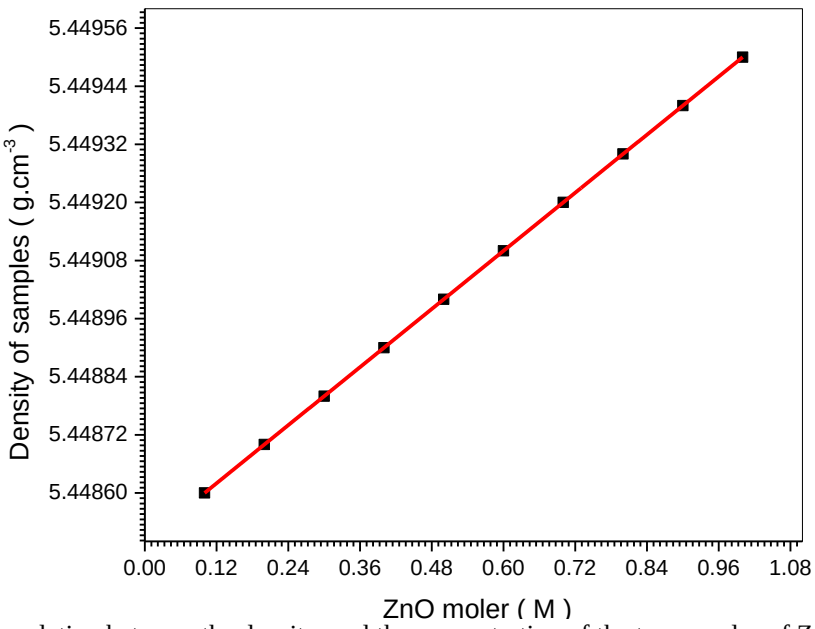

Figure(2) : The relation between the density and the concentration of the ten samples of ZnO thin filims.

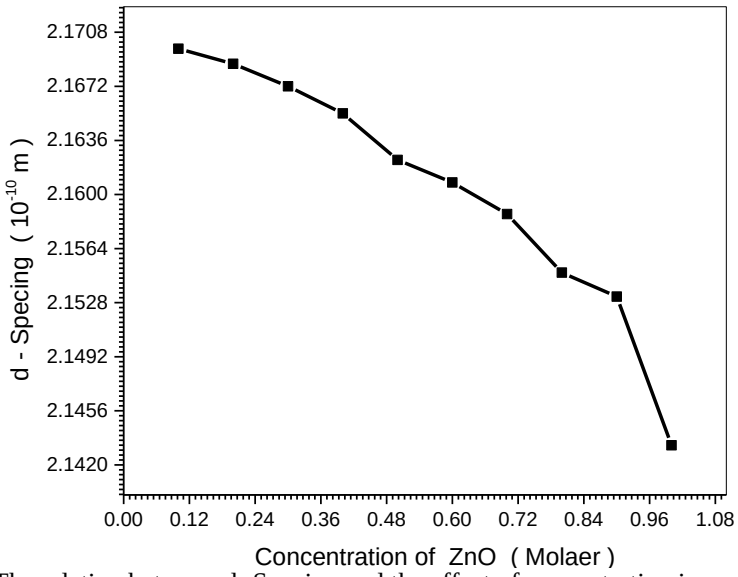

Figure (3): Indicate The relation between d- Specing and the effect of concentration in as-syntheized ZnO thin filims nanoparticles.

The chamical constitutions of ZnO nanostructures were examined through Mattson Fourier Transform Infrared Spectrophotometer (FTIR) in the range of 400 to 4000 cm^{-1} at room temperature Fig(4) . The infrared spectra of all ZnO nanosample were recorded for all samples, the bands around 455 and 850 cm^{-1} are assigned to the metal-oxygen vibration in the tetrahedral sides. The difference in the spectral positions is due to the different values of metal ion-O^{-2} distances for octahedral and tetrahedr sites. The band around 1205 is due to C-C stretching vibration and C-C-H bending vibration. The band around 1340 cm^{-1} is associated with the O-H bending vibration .The band around 2450 cm^{-1} is due to C=C stretching. The bands around 3640$cm^{-1}$and 3910 cm^{-1} respecively are due to the stretching mode of H-O-H bending vibration of free or absorbed water which implies that the hydroxyl groups are retained in ZnO of different concentration of zinc acetate.

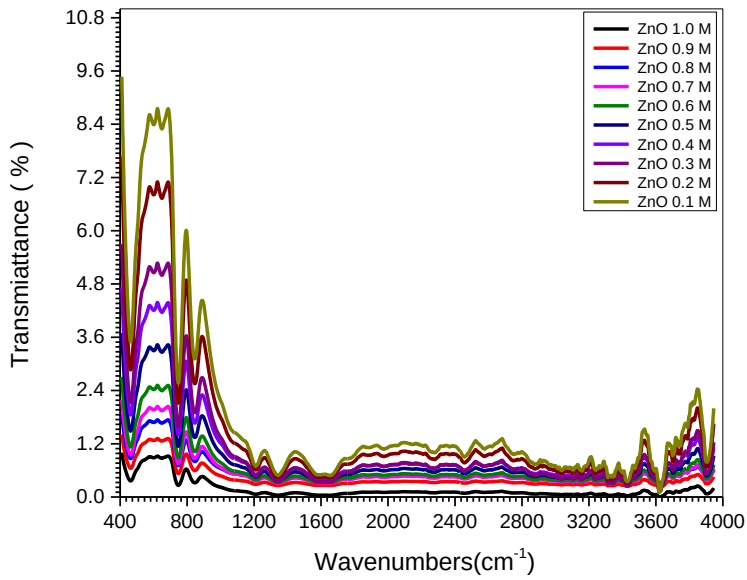

Figure (4): demonstrate FTIR spectrum of the ten samples of as- obtained ZnO nanostructures.

The optical conductivity is a measure of frequency response of material when irradiated with light which is determined using the following relation [23]:

$$\boldsymbol{\delta_{opt}} = \frac{\alpha n c}{4\pi} \qquad \textbf{(1)}$$

Where(c) is the light velocity, $\boldsymbol{\delta_{opt}}$ is optical condictivity, n is refrective index and $\boldsymbol{\alpha}$ is the obsorption cofficient. The electrical conductivity can be estimated using the following relation [41]:

$$\delta_{ele} = \frac{2\lambda\delta_{opt}}{\alpha}. \qquad (2)$$

Where λ is the wavelengt. The high magnitude of optical conductivity is about $1.34x10^{11}$ sec^{-1} noticed in Figure (5) which confirms the presence of very high photo-response for samples 1.0, 0.9 and 0.8 molar respectively of as-prepared ZnO nanostructures. The increase of optical conductivity at high photonenergies is due to the high absorbance of as-prepared samples ZnO at different molars and also may attributed to electron excitation by photon energy. Moreover, Figure 6 indicates that the interception carves on y-axix show low electrical condictivity for high concentration in comporison with other and this may atrributed to higher band gab at higher molar concentraton of ZnO/film [23].

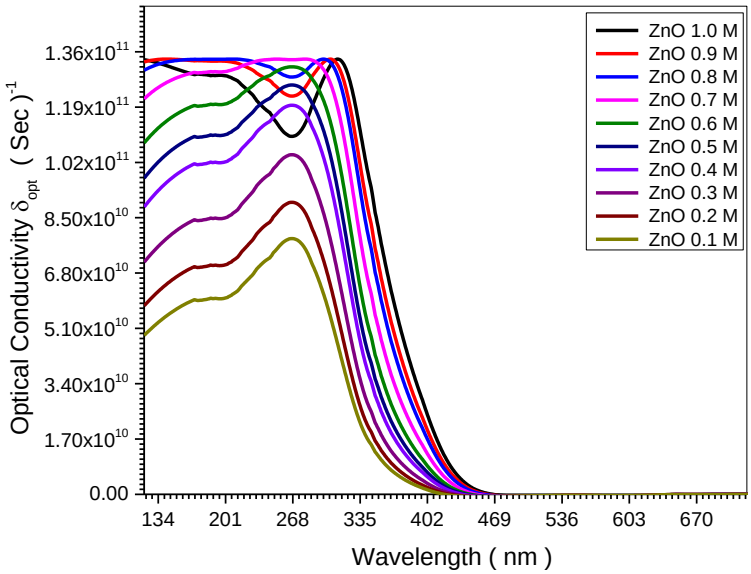

Figure (5): shows the relation between the optical conductivity and wavelengths of ten samples of as-synthezied ZnO nanostructures.

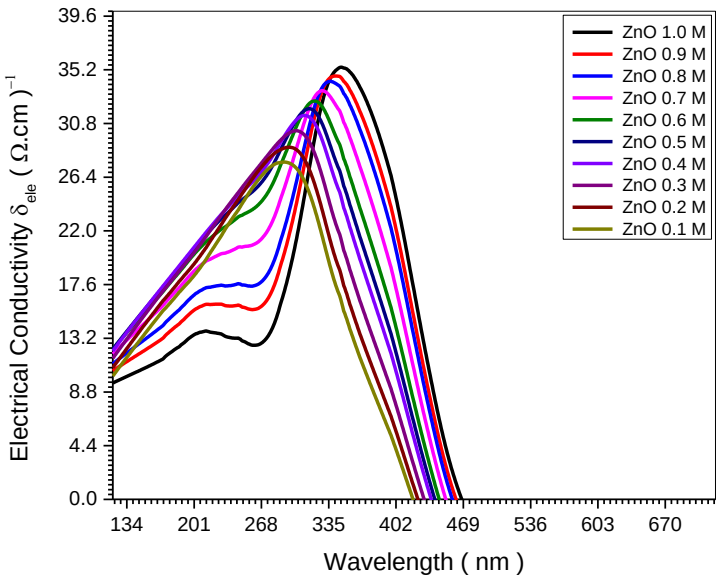

Figure (6): Illustrates the relation between the electrical conductivity and wavelengths of the ten samples of as-synthezied ZnO nanostructures.

IV. Conclusions

In this paper ,we have reported the effect of different concentrations of zinc-acetate on the structural and the electrical conductivity of ZnO/films nanostructures. The XRD patterns exhibited that all samples of ZnO nanostructures synthesized at different concentration of zinc acetate confirmed the formation of spinal Cubic crystal using sol-gel method. The band around 1340 cm^{-1} is associated with the O-H bending vibration . The result also show that, the increasing in the concentration of zinc acetate lead to increase in the density (δ) of

ZnO nanoparticles by rate 10^{-3}(g.cm^{-3}) and decreasing the d-spacing by rate (0.026 ^{o}A .mol^{-1}). Moreover, the results confirmed that low electrical condictivity match the high concentration zinc acetate.

References

[1]. U. Ozgur, Ya I. Alivov, C. Liu, A. Teke, M.A. Reshchikov, S. Dog˘an, V. Avrutin, S.-J.Cho, H. Morkoc, A comprehensive review of ZnO materials and devices, J. Appl.Phys. 98 (2005) 041301.

[2]. J. Yu, X. Yu, Hydrothermal synthesis and photocatalytic activity of zinc oxide hollow spheres, Environ. Sci. Technol. 42 (2008) 4902–4907.

[3]. O. Seven, B. Dindar, S. Aydemir, D. Metin, M.A. Ozinel, S. Icli, Solar photocatalytic disinfection of a group of bacteria and fungi aqueous suspensions with TiO2, ZnO and Sahara desert dust, J. Photochem. Photobiol. A Chem. 165 (2004) 103–107.

[4]. O. Yamamoto, Influence of particle size on the antibacterial activity of zinc oxide, Int. J. Inorg. Mater. 3 (2001) 643–646.

[5]. R. Brayner, R. Ferrari-Illiou, N. Briviois, S. Djediat, M.F. Benedetti, F. Fievet, Toxicological impact studies based on Escherichia coli bacteria in ultrafine ZnO nanoparticles colloidal medium, Nano Lett. 6 (2006) 866–870.

[6]. N.M. Franklin, N.J. Rogers, S.C. Apte, G.E. Batley, G.E. Gadd, P.S. Casey, Comparative toxicity of nanoparticulate ZnO, Bulk ZnO, and ZnCl2 to a freshwater microalga (Pseudokirchneriella subcapitata): the importance of particle solubility, Environ. Sci. Technol. 41 (2007) 8484–8490.

[7]. N. Talebian, M.R. Nilforoushan, E. Badri Zargar, Enhanced antibacterial performance of hybrid semiconductor nanomaterials: ZnO/SnO2 nanocomposite thin films, Appl. Surf. Sci. 258 (2011) 547–555.

[8]. J. Sawai, S. Shoji, H. Igarashi, A. Hashimoto, T. Kokugan, M. Shimizu, H. Kojima, Hydrogen peroxide as an antibacterial factor in zinc oxide powder slurry, J.Ferment. Bioeng. 86 (1998) 521–522.

[9]. S. Atmaca, K. Gul, R. Clcek, The effect of zinc on microbial growth, Turk. J. Med. Sci. 28 (1998) 595–597.

[10]. H.C. Poynton, J.M. Lazorchak, C.A. Impellitteri, M.E. Smith, K. Rogers, M. Patra, K.A. Hammer, H.J. Allen, C.D. Vulpe, Differential gene expression in Daphnia magna suggests distinct modes of action and bioavailability for ZnO nanoparticles and Zn ions, Environ. Sci. Technol. 45 (2011) 762–768.

[11]. K.H. Tam, A.B. Djurišic, C.M.N. Chan, Y.Y. Xi, C.W. Tse, Y.H. Leung, W.K. Chan,F.C.C. Leung, D.W.T. Au, Antibacterial activity of ZnO nanorods prepared by a hydrothermal method, Thin Solid Films 516 (2008) 6167–6174.

[12]. Kim K, Moon T, Lee M, Kang J, Jeon Y, Kim S: Light-emitting diodes composed of n-ZnO and p-Si nanowires constructed on plastic substrates by dielectrophoresis. Solid State Sci, 13 (2011) 1735–1739.

[13]. Kim H, Gilmore CM, Transparent conducting aluminum-doping zinc oxide thin filims for organc light emitting devices , Appl. Phys. Lett., 76 (2000) 259-264.

[14]. Foo KL, Kashif M, Hashim U, Ali M: Fabrication and characterization of ZnO thin films by sol–gel spin coating method for the determination of phosphate buffer saline concentration. Curr Nanosci, 9 (2013) 288–292.

[15]. Guillen E, Azaceta E, Peter LM, Zukal A, Tena-Zaera R, Anta JA: ZnO solar cells with an indoline sensitizer: a comparison between nanoparticulate films and electrodeposited nanowire arrays. Energy Environ Sci 2011, 4:3400–3407.

[16]. Chai G, Lupan O, Chow L, Heinrich H: Crossed zinc oxide nanorods for ultraviolet radiation detection. Sensor Actuat A Phys 2009, 150:184–187.

[17]. Fulati A, Ali SMU, Asif MH, Alvi NH, Willander M, Brännmark C, Strålfors P, Börjesson SI, Elinder F, Danielsson B: An intracellular glucose biosensor based on nanoflake ZnO. Sensor Actuat B Chem 2010, 150:673–680.

[18]. Li YB, Bando Y, Sato T, Kurashima K: ZnO nanobelts grown on Si substrate. ppl Phys Lett 2002, 81:144–146.

[19]. Lee W, Sohn H, Myoung JM: Prediction of the structural performances of ZnO nanowires grown on GaAs (001) substrates by metalorganic chemical vapour deposition (MOCVD). Mater Sci Forum 2004, 449–452:1245–1248.

[20]. Karami H, Fakoori E: Synthesis and characterization of ZnO nanorods based on a new gel pyrolysis method. J Nanometer 2011, 2011:11.

[21]. Kaneva N, Dushkin C: Preparation of nanocrystalline thin films of ZnO by sol–gel dip coating. Bulg Chem Commun 2011, 43:259–263.

[22]. Yi S-H, Choi S-K, Jang J-M, Kim J-A, Jung W-G: Low-temperature growth of ZnO nanorods by chemical bath deposition. J Colloid Interface Sci 2007, 313:705–710.

[23]. A.F. Masnsour et al, Improvement Structural and opitical properties of ZnO/PVA Nanocomposites, Journal of Applied Physics, 7(2015) 60-69.

IOSR Journal of Applied Physics (IOSR-JAP) is UGC approved Journal with Sl. No. 5010, Journal no. 49054.

A. B. Awatif " Effect of Different Concentrations of Zinc Acetate on the Structural, and the Optical and the Electrical Conductivity of ZNO Nanostructures." IOSR Journal of Applied Physics (IOSR-JAP), vol. 11, no. 6, 2019, pp. 35-40.